the

meteorological

magazine

Cloud types for Observers

This publication has been prepared in the Meteorological Office, and is attractively produced on stout card of convenient size, being designed for outdoor as well as indoor use. It contains 37 photographs with descriptive notes which will help the observer to identify the main types of cloud. Additional notes, diagrams and coding instructions are also included to enable the observer to classify the state of the sky in accordance with the codes approved by the World Meteorological Organization.

This album replaces the earlier publications *Cloud Forms and Cloud card for observers*, which are now obsolete because of changes in cloud classification introduced by the World Meteorological Organization.

10s 6d (by post 11s 4d)

Published by

Her Majesty's Stationery Office

and obtainable from the Government Bookshops in London (post orders to PO Box 569, SE1), Edinburgh, Cardiff, Belfast, Manchester, Birmingham and Bristol, or through any bookseller

551.576.4:629.7.08

ON THE REPRESENTATIVENESS OF MEASUREMENTS OF HEIGHT OF LOW-CLOUD BASE AT AN AIRFIELD

By L. S. CLARKSON

Summary. Routine observations of cloud base are made at half-hour intervals at each of two sites 3 km apart at Liverpool Airport. Cloud-base recorders are available at each site. During January, March and May 1969 a note was made, for each site, of the lowest cloud height recorded in the 10 minutes previous to the routine weather observations.

If H_x represents the lowest height of cloud base in the range 100–700 ft recorded at one site in a 10-minute period and if H_3 represents the lowest height recorded in the appropriate 10-minute period at another site 3 km away, then at Liverpool Airport these are statistically related by an equation very close to

$$H_3 = 0.76\,H_x + 170\text{ ft,}$$

with a standard error of estimate of 320 ft.

The percentage of occasions when H_3 is 0.5 H_x or less varies from 27 per cent when $H_x = 100$ ft to 16 per cent when $H_x = 700$ ft.

Introduction. At Liverpool Airport records were examined from two properly maintained cloud-base recorders (CBR) in routine operational use. One is situated in the south-east corner of the airport near the meteorological observing office; the other is about 3 km away in the north-west corner adjacent to the forecast office.

It is thought that an observer making a routine height of cloud-base observation for aviation is considerably influenced by the lowest height that has been recorded in the 10-minute period immediately prior to the time of observation. Accordingly, the staff at Liverpool Airport Meteorological Office were asked to extract the lowest height recorded at each location at any time within the 10-minute period before every half-hourly routine observation, provided that a height at or below 1000 ft was shown on either recorder in this time interval. Heights were read off to the nearest 20 ft for cloud bases below 1000 ft, and F or — was entered when either fog or no cloud base was recorded. Data tabulated in this way for the months of January, March and May 1969 were analysed.

Analysis. The lowest cloud height recorded at the forecast office site was represented by H_f and the lowest cloud height recorded in the same 10-minute period at the observing office site was represented by H_o.

There were (see Table I) 352 pairs of observations of H_f and H_o in which H_f was in the range 100–700 ft. (The value of H_o when it was tabulated as F or — was taken as being zero (i.e. on the surface) if this could reasonably be deduced from the immediately preceding or following half-hourly observation.)

Similarly there were 379 pairs of observations of H_o and H_f in which H_o was in the range 100–700 ft. (In these pairs the value of H_f when it was tabulated as F or — was taken as being zero if this could reasonably be deduced from the immediately preceding or following half-hourly observation.)

The two separate regression equations (of H_o on $H_{f\,(100\text{-}700)}$ and of H_f on $H_{o\,(100\text{-}700)}$) were formed, where the notation $H_{f\,(100\text{-}700)}$ refers to observations in the range 100–700 ft. The 'standard errors of estimate' and correlation coefficients were calculated, with the results shown in Table I below.

TABLE I—STATISTICAL RELATIONSHIPS BETWEEN H_o AND H_f

Number of pairs of observations	Regression equation *feet*	Standard error	Correlation coefficient
352	$H_o = 0 \cdot 76\, H_{f(100-700)} + 151$	309	0·34
379	$H_f = 0 \cdot 76\, H_{o(100-700)} + 187$	326	0·34

Discussion. From the near identity of the constants in the two regression equations it appears that, over the range of cloud heights considered, any constant systematic difference between the lowest cloud heights recorded at the two sites is negligibly small.

The low value of the correlation coefficient between H_o and H_f and the high 'standard error of estimate' of the cloud base 3 km away from an observation of the height of low cloud in the range 100–700 ft are noteworthy.

If H_x represents the lowest height of cloud base in the range 100–700 ft recorded at one site in a 10-minute period, and if H_s represents the lowest height of cloud base recorded within the same 10-minute period at a spot 3 km distant, then at Liverpool Airport these are statistically related by an equation very close to

$$H_s = 0 \cdot 76\, H_x + 170 \text{ ft,} \qquad \qquad \cdots (1)$$

with standard error of estimate 320 ft.

Equation (1) is expressed in graphical form in Figure 1, where the upper and lower dotted lines represent the 50 per cent confidence limits of the regression line AB of H_s on H_x. The dashed line CD is the regression line to be expected when the differences between the observations at H_x and H_s are evenly distributed about a mean difference of zero. It departs increasingly from the computed regression line AB as H_x decreases. This is because whereas there is no physical constraint on the possible values of H_s when H_s is greater than H_x, the presence of the ground puts a lower limit to the range of physically possible values of H_s when H_x is small.

The standard error of estimate of H_s from H_x is considerably larger than the value for Heathrow obtained by Harrower using two cloud searchlights in 1955 (unpublished) and quoted by Jones.* This is probably because the observations analysed by Harrower were made simultaneously, and restricted

---

* JONES, R. F.; Time and space variations of visibility and low cloud within the approach control area. *Tech. Note Wld met. Org.*, Geneva, 1969, No. 95, pp. 97–101.

to more than 4/8 of cloud with bases below 300 ft at *both* sites, whereas the range of the observations at the distant site analysed in this note is not artificially limited.
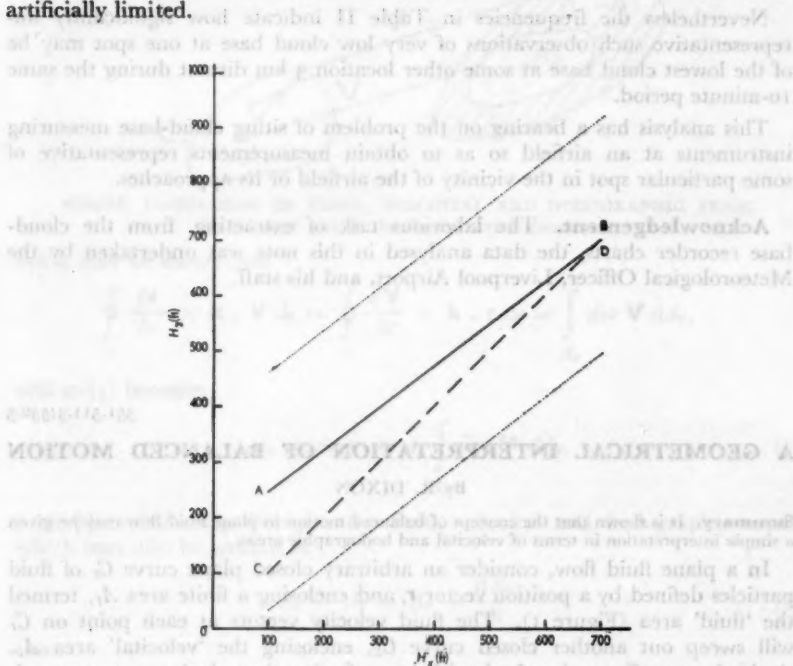

FIGURE I—REGRESSION OF H_3 ON H_x AND 50 PER CENT CONFIDENCE LIMITS

AB   Regression of H_3 on H_x.
CD   Regression line to be expected when the differences between the observations
      of H_x and H_3 are evenly distributed about a mean difference of zero.
.... 50 per cent confidence limits.

From the statistical relationship found between the observations of H_3 and H_x at Liverpool Airport as expressed by equation (1), it is possible to draw up Table II which, for specified values of H_x, expresses the probable frequency of occasions when H_3 is $0.5 H_x$ or less.

TABLE II—FREQUENCY OF OCCASIONS WHEN H_3 IS $0.5 H_x$ OR LESS

H_x feet	$H_3 \leqslant 0.5 H_x$ percentage of occasions
100	27
300	22
500	17
700	16

It must be remembered that the observations H_3 and H_x are not necessarily simultaneous, nor are they time-meaned; they are in fact the instantaneous heights of the lowest cloud recorded by the cloud-base recorders at the two sites during the same 10-minute time intervals. Consequently they must include some instances where the CBR at either or both sites picked up an

isolated fragment of very low cloud which chanced to be vertically above the receiver at the moment of scanning.

Nevertheless the frequencies in Table II indicate how significantly unrepresentative such observations of very low cloud base at one spot may be of the lowest cloud base at some other location 3 km distant during the same 10-minute period.

This analysis has a bearing on the problem of siting cloud-base measuring instruments at an airfield so as to obtain measurements representative of some particular spot in the vicinity of the airfield or its approaches.

Acknowledgement. The laborious task of extracting, from the cloud-base recorder charts, the data analysed in this note was undertaken by the Meteorological Officer, Liverpool Airport, and his staff.

A GEOMETRICAL INTERPRETATION OF BALANCED MOTION

By R. DIXON

Summary. It is shown that the concept of balanced motion in plane fluid flow may be given a simple interpretation in terms of velocital and hodographic areas.

In a plane fluid flow, consider an arbitrary closed plane curve C_r of fluid particles defined by a position vector $\mathbf{r}$, and enclosing a finite area A_r, termed the 'fluid' area (Figure 1). The fluid velocity vectors at each point on C_r will sweep out another closed curve C_v, enclosing the 'velocital' area A_v. A third curve C_h can be obtained by transferring the velocity vector at each point of C_r to the origin. This curve C_h encloses the 'hodographic' area A_h.

Now the three areas A_r, A_v, A_h are given by

$$2A_r = \oint_c \frac{\partial \mathbf{r}}{\partial c} \times \mathbf{k} \cdot \mathbf{r} \, dc, \qquad \ldots (1)$$

$$2A_v = \oint_c \frac{\partial}{\partial c} (\mathbf{r} + \mathbf{V}) \times \mathbf{k} \cdot (\mathbf{r} + \mathbf{V}) dc, \qquad \ldots (2)$$

$$2A_h = \oint_c \frac{\partial \mathbf{V}}{\partial c} \times \mathbf{k} \cdot \mathbf{V} \, dc, \qquad \ldots (3)$$

where $\mathbf{V}$ is the velocity, dc is an element of C_r and $\mathbf{k}$ is the unit vector at right angles to the plane.

By multiplying out the integrand in (2), and using (1) and (3) there follows

$$2A_v = 2A_r + 2A_h + \oint_c \frac{\partial \mathbf{r}}{\partial c} \times \mathbf{k} \cdot \mathbf{V} \, dc + \oint_c \frac{\partial \mathbf{V}}{\partial c} \times \mathbf{k} \cdot \mathbf{r} \, dc; \qquad \ldots (4)$$
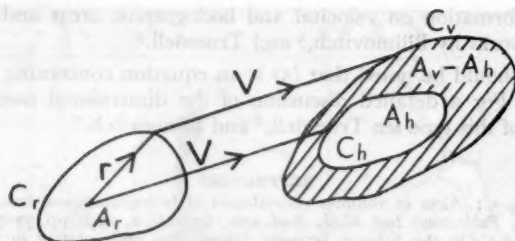
FIGURE 1—DIAGRAM OF FLUID, VELOCITAL AND HODOGRAPHIC AREAS
In balanced motion the shaded area is conserved.

but it may be shown that

$$\oint_c \frac{\partial \mathbf{r}}{\partial c} \times \mathbf{k} \cdot \mathbf{V} \, dc = \oint_c \frac{\partial \mathbf{V}}{\partial c} \times \mathbf{k} \cdot \mathbf{r} \, dc = \int_{A_r} \operatorname{div} \mathbf{V} \, dA_r,$$

and so (4) becomes

$$A_v = A_r + A_h + \int_{A_r} \operatorname{div} \mathbf{V} \, dA_r, \qquad \ldots (5)$$

a simple relationship between the fluid, velocital and hodographic areas, which may also be written as

$$A_v = A_r + A_h + \frac{dA_r}{dt} \qquad \ldots (6)$$

since

$$\frac{dA_r}{dt} = \int_{A_r} \operatorname{div} \mathbf{V} \, dA_r . \qquad \ldots (7)$$

In deriving the relationship between the velocity field and the mass field in balanced flow in meteorology, the conditions

$$\frac{d}{dt} (\operatorname{div} \mathbf{V}) = \operatorname{div} \mathbf{V} = 0 \qquad \ldots (8)$$

have been imposed. Consequently by taking the rate of change of (5), and using Reynolds's Transport Theorem

$$\frac{d}{dt} \int_{A_r} \operatorname{div} \mathbf{V} \, dA_r = \int_{A_r} \left[\frac{d}{dt} (\operatorname{div} \mathbf{V}) + (\operatorname{div} \mathbf{V})^2 \right] dA_r \qquad \ldots (9)$$

and equations (7) and (8), there results

$$\frac{d}{dt} (A_v - A_h) = 0, \qquad \ldots (10)$$

or in other words, in balanced motion, the area between the curves C_v and C_h, is conserved. Thus the term 'balanced' motion is geometrically as well as dynamically apposite.

Further information on velocital and hodographic areas and volumes can be found in works by Bilimovitch,[1] and Truesdell.[2]

Finally, it should be noted that (5) is an equation concerning the geometry of Figure 1. For a detailed discussion of the dimensional non-homogeneity of equations of this type see Truesdell,[2] and Bilimovitch.[3]

REFERENCES

1. BILIMOVITCH, A.; Aires et volumes vélocidiques et hodographiques dans un mouvement du fluide. *Publs scient. Inst. Math. Acad. serbe, Belgrade,* 2, 1948, pp. 37–52.
2. TRUESDELL, C.; On the balance between deformation and rotation in the motion of a continuous medium. *Jnl Wash. Acad. Sci., Washington,* 40, 1950, pp. 313–317.
3. BILIMOVITCH, A.; Sur l'homogénéisation des équations de nature vélocidique. *Publs scient. Inst. Math. Acad. serbe, Belgrade,* 5, 1953, pp. 20–34.

551.575.1

RADIATION FOG CLEARANCE AT LITTLE RISSINGTON

By J. HOUSEMAN

Summary. Various workers have formulated empirical rules for forecasting the clearance time of radiation fog at low-lying stations in East Anglia, and in some cases an allowance for upslope motion has been incorporated. An examination was made of 215 fogs which occurred during a recent 3-year period at Little Rissington, an airfield at 750 ft above mean sea level. The fogs were classified and the empirical rules for East Anglia were applied to 87 radiation type fogs. Only 19 fogs cleared before the forecast time of clearance so a special allowance for upslope motion was made to bring the forecast time as near as possible to the actual time of clearance for the maximum number of cases. The results indicate that even at Little Rissington with its unusual exposure the empirical rules can be modified with some success to meet local peculiarities.

Introduction. Over the past few years extensive use has been made of Barthram's diagrams[1] for forecasting the time of clearance of radiation fog by Kennington's method.[2] Atkins[3] has formulated empirical rules for calculating fog thickness and allowing for upslope motion at Wittering and these rules have been tested at Gaydon, Cottesmore and Watton[4] with varied success.

It was thought that it would be of interest to test Atkins's rules at an airfield, considerably higher than any of those mentioned above, where virtually all fog is affected by upslope motion, in order, if possible, to devise a series of adjustments to the basic method to provide a useful local forecasting tool.

The particular airfield, Little Rissington, lies on the top of a Cotswold hill at an elevation of 750 ft (approximately 230 m) above mean sea level. Only on the north-west does the crest of the hill overlook the airfield and beyond this low crest the ground falls away steeply for some 200 ft (approximately 60 m). In all other directions the hillside slopes steeply away from the airfield boundary. Consequently all air approaching the airfield at ground level is subject to an upslope effect in varying degree (see Figure 1).

Observations of all fogs affecting the airfield during the period 1 January 1965 to 31 December 1967 were examined, some 215 cases in all. Individual fogs persisted for periods of time varying from as little as one hour to as much as four and a half days.
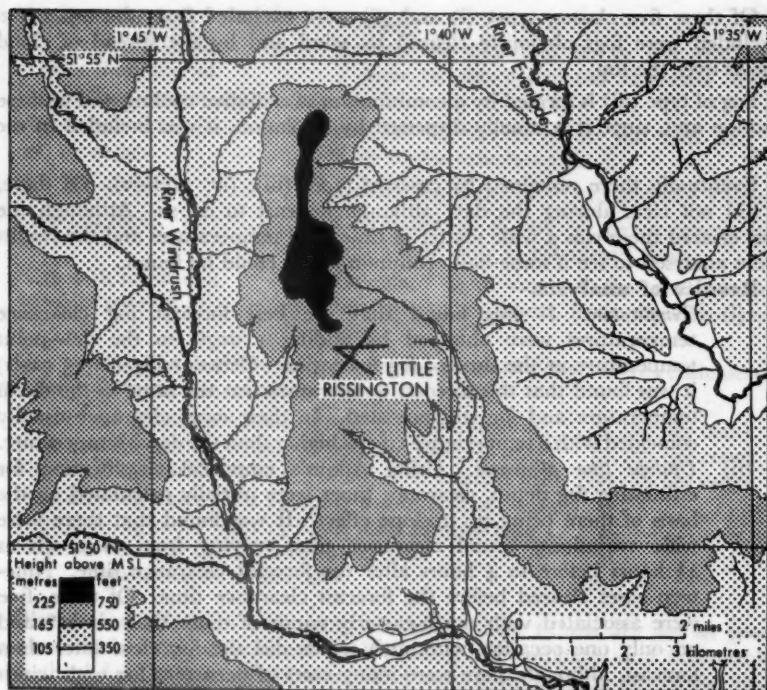
FIGURE I—MAP SHOWING LITTLE RISSINGTON AND ITS SURROUNDINGS

A preliminary investigation showed that, broadly speaking, the fogs fell into five categories, as follows :

(i) Advection fog which formed widely both on high and low ground in warm, moist air masses.

(ii) Hill fog which, over low ground, was reported as low stratus cloud.

(iii) Fog which formed on clear, radiation nights with some wind. This type often began as an isolated patch of status over the hill, gradually lowering as the wind decreased, to form fog. Sometimes fog also formed in the surrounding valleys but at other times they remained clear.

(iv) Radiation fog which formed first in the valleys and gradually increased in depth to envelop the hilltop.

(v) Radiation fog which formed in the valleys by night, leaving the hilltop clear, but which lifted during the following morning to form stratus over the valleys and fog on the hill before finally dispersing.

Of these five classes, types (i) and (ii) were excluded from the test. Also excluded were fogs obviously cleared by wind and by the spread of cloud sheets over the top.

Fog of type (iii) is formed by a combination of radiative cooling and upslope motion and, since it is usually dispersed by insolation, it was included in the test.

Eventually there remained 87 cases of types (iii), (iv) and (v). Of these, 6 did not clear during the day, although forecast to do so. Although the rest cleared there was a wide scatter of times and temperatures and the results were analysed to see if some basic common factor could be found.

Results of analysis.

(i) *Temperature.* It was found that the best forecast fog clearance temperatures were obtained by adding 1 degC to the dew-point temperature at the time of fog formation. Occasionally (in 13 cases) it was found that this forecast temperature was the same as the dawn temperature and fog still persisted. In these cases clearance usually coincided with a temperature 1 degC higher than the dawn temperature.

(ii) *Upslope time allowance.* Using Atkins's empirical classification for estimating fog depth, clearance times were initially calculated on the basis of there being no upslope effect. It was found that there were wide variations, actual clearance time varying from as much as 4½ hours before to 4 hours after the forecast clearance time. Nineteen cases cleared before the forecast clearance time. Of these, five were associated with north-easterly winds of more than 10 kt* and on only one occasion with such winds did the fog clear later than forecast, although there were many cases of persistent fog with winds of over 10 kt from other directions. Six of the remaining 14 cases had clearance times within the half hour preceding the forecast time.

All the other fogs cleared after the forecast clearance time. Excluding the 6 which did not clear at all that day, there were 62 cases which cleared later than forecast, whereas only 19 cleared earlier than forecast. Therefore, to bring the forecast clearance time as near as possible to the actual clearance time in the maximum number of cases, an allowance was added to all the basic forecast clearance times which had been calculated, except those involving north-east winds of over 10 kt. The allowance was calculated on the basis of obtaining the best results with specific types of fogs. It was found that the allowance did not need to vary with the time of the year and that Atkins's allowances were usually too large, especially (and rather surprisingly) in the case of freezing fogs. The following rules for calculating radiation fog clearance temperatures and times were eventually formulated.

Forecast clearance temperature.

(i) Take the dew-point at the time of fog formation and add 1 degC.

(ii) If this temperature turns out to be the dawn temperature add another 1 degC and recalculate the clearance time.

Forecast clearance time. Calculate this in accordance with the following rules using Barthram's diagrams and the temperature already forecast.

---

* 1 knot ≈ 0·5 m/s.

Description of fog	Procedure
Sky visible. Visibility greater than 200 yd (approximately 185 m).	Assume fog depth to be 10 mb and add ½ hour to the calculated clearance time.
Sky visible. Visibility 200 yd or less.	Assume fog depth of 20 mb and add 1 hour to the calculated time.
Sky not visible.	Assume fog depth of 30 mb and add 1 hour.
Freezing fogs.	Calculated as if one of above types, but add ½ hour only to calculated time.
Fogs with north-east winds of over 10 kt.	Calculate as if one of the above types but *subtract* 1½ hours from the calculated time.

On the basis of the above rules all the fog clearance times were recalculated and the results were as follows :

Fogs clearing within ½ hour of adjusted forecast time	34	(39 per cent)
Fogs clearing within 1 hour of adjusted forecast time	57	(66 per cent)
Fogs clearing within 1½ hours of adjusted forecast time	68	(78 per cent)
Fogs clearing more than 1½ hours before forecast time	7	
Fogs clearing more than 1½ hours after forecast time	6	
Fogs not clearing though forecast to clear	6	
Total number of forecasts	87	

Discussion. From a forecasting viewpoint these results are not as good as those which Atkins achieved at Wittering but compare very favourably with those for Gaydon and Watton. The most disappointing aspect was that none of the 'nil clearances' could be successfully forecast and no common factor was apparent either in those cases or in those which cleared very late. Nevertheless it seems that investigations such as this can be of value even at stations with an unusual exposure.

REFERENCES

1. BARTHRAM, J. A.; A diagram to assess the time of fog clearance. *Met. Mag., London*, **93**, 1964, pp. 51–56.
2. KENNINGTON, C. J.; An approach to the problem of the forecasting of fog clearances. *Met. Mag., London*, **90**, 1961, pp. 70–73.
3. ATKINS, N. J.; Forecasting fog clearance at Wittering. *Met. Mag., London*, **94**, 1965, pp. 298–300.
4. JENNINGS, T. D. D., MACEY, C. J. and GILES, B. L.; Forecasting fog clearance at Gaydon, Cottesmore and Watton. *Met. Mag., London*, **94**, 1965, pp. 301–302.

INTRODUCTION TO THE FAST FOURIER TRANSFORM (FFT) IN THE PRODUCTION OF SPECTRA

By R. RAYMENT

Summary. The existence of a powerful technique, generally referred to as the Fast Fourier Transform (FFT), for evaluating Fourier coefficients is presented and the use of this in the production of spectra is explained. A basis for choice between this comparatively new method and a much used conventional technique for producing spectra is put forward and some other uses of the FFT are briefly indicated.

Nomenclature.

$a_o/2$	Mean level of a function represented by a Fourier series.
$\left.\begin{array}{c} a_k, b_k \\ c_k, d_k \end{array}\right\}$	Fourier amplitudes or coefficients.
C_k	Complex Fourier amplitude $= (a_k + ib_k)/2$.
C_{-k}	Complex Fourier amplitude $= (a_k - ib_k)/2$.
D_k, D_{-k}	Complex Fourier amplitudes for a second function.
g	Number of lags in the Blackman and Tukey (B&T) method.
H	Number of spectrum points averaged in the Fast Fourier Transform (FFT) method.
j	Running time index (i.e. $t = j\Delta t$).
k	Running frequency index for the Fourier series (i.e. $n = k/T$), for the FFT (i.e. $n = k\Delta n$) and for the B&T method (i.e. $n = k/2g\Delta t$).
L	Time span index for a lag in the B&T method (i.e. $\tau = L\Delta t$).
n	Frequency.
N	Total number of measured points in one sample of data.
$O(\tau), E(\tau)$	Odd and even parts respectively of the cross-correlation (i.e. $\sigma_{xy}(\tau) = O(\tau) + E(\tau)$).
$Q_{xy}(n)$	Quadrature spectrum function.
$S_{xy}(n)$	Cospectrum function.
$S_x(n)$	Power spectrum function.
t	Time.
u', w', θ'	Fluctuations in the horizontal wind, vertical wind and temperature respectively.
$x(t), y(t)$	Functions of time.
Δt	Time interval between measured data points.
Δn	Fundamental frequency interval $(= 1/T)$.
v	Degrees of freedom
$\sigma_{xy}(\tau)$	Cross-correlation or cross-product between $x(t)$ and $y(t)$ for a lag of τ.
$\sigma_x(\tau)$	Autocorrelation for $x(t)$.
τ	Lag used in deriving cross-products.
T	Periodic time or total sampling time.
$\varphi_{xy}(n)$	Complex spectral density function.
χ^2	Chi-square probability distribution.
δn	Bandwidth in B&T method.

Introduction. The requirement to produce spectra arises whenever one needs to know which set of repetition rates or frequencies dominate some particular process.

As an illustration of the use of spectra suppose we have a measure of the variance of the wind $\sigma_v{}^2$. Such a measurement is inevitably made from discrete observations separated by a time interval Δt say, over a limited time, say T, using an instrument with a less than perfect response characteristic. Roughly it is clear that if there are significant wind motions which have a frequency greater than the maximum response of the instrument and/or a frequency less than $1/T$ the calculated $\sigma_v{}^2$ could be much in error. Spectral analysis of the wind can show which frequencies contribute most to the variance.

If there is good reason for expecting a certain shape to the spectral curve the analysis can indicate whether the recording time is long enough and, provided Δt is short enough, whether the instrumental response is adequate. This is just one example and a few more will be quoted further on.

Classical harmonic analysis. The classical way of considering the discrete frequencies associated with some process is to visualize this as made up from the superposition of a set of sinusoidal components having different frequencies and amplitudes. This idea is expressed mathematically by expanding the describing function, $x(t)$, in terms of the so-called **Fourier components** :

$$x(t) = \frac{a_o}{2} + \sum_{k=1}^{\infty} (a_k \cos (2\pi kt/T) + b_k \sin (2\pi kt/T)) \qquad \ldots (1)$$

where a_k and b_k are the Fourier amplitudes or coefficients and $x(t)$ might be a signal generated in time over a period of T. In complex form (1) may be written :

$$x(t) = \sum_{k=-\infty}^{\infty} C_k \exp (-2\pi ikt/T) \qquad \ldots (2)$$

where

$$C_k = \frac{1}{T} \int_0^\infty x(t) \exp (2\pi ikt/T) \, dt = (a_k + ib_k)/2. \qquad \ldots (3)$$

We shall also need a second function :

$$y(t) = \sum_{k=-\infty}^{\infty} D_k \exp (-2\pi ikt/T) \qquad \ldots (4)$$

where

$$D_k = (c_k + id_k)/2, \quad D_{-k} = (c_k - id_k)/2 \text{ etc.} \qquad \ldots (5)$$

For the purposes of defining a spectrum we introduce the average cross-correlation (cross-product) for signals of zero mean, which can be written as

$$\sigma_{xy}(\tau) = \frac{1}{T} \int_0^T x(t) \, y(t - \tau) dt, \qquad \ldots (6)$$

which is periodic in T and where τ is the lag of one function on the other. From theorems due originally to Wiener[1] (see also Taylor[2] and Lumley and Panofsky[3]) we can express the cross-correlation in terms of a complex frequency or spectral density function $\varphi_{xy}(n)$;

$$\sigma_{xy}'(\tau) = \int_{-\infty}^{\infty} \varphi_{xy}(n) \exp{(2\pi i n\tau)} dn \qquad \dots (7)$$

where n is the frequency.

We require at zero lag the covariance given by

$$\sigma_{xy}(0) = \int_{-\infty}^{\infty} \mathrm{Re}\varphi_{xy}(n) dn = \int_{0}^{\infty} S_{xy}(n) dn \qquad \dots (8)$$

where $\mathrm{Re}\varphi_{xy}(n)$ is the real part of $\varphi_{xy}(n)$, and since $\mathrm{Re}\varphi(n)$ is symmetrical, $S_{xy}(n) = 2\mathrm{Re}\varphi_{xy}(n)$ where $S_{xy}(n)$ gives the contribution to the covariance from different frequencies and is called the cospectrum.

In the atmosphere if one were measuring horizontal and vertical velocity fluctuations, i.e. u' and w' respectively, $\sigma_{u'w'}(0)$ is directly proportional to the turbulent momentum flux. Similarly if temperature fluctuation (i.e. θ') are measured $\sigma_{w'\theta'}(0)$ is proportional to the turbulent heat flux.[3]

There is also a quantity $Q_{xy}(n)$ which measures the $\pi/2$ out-of-phase intensity of the two signals and is called the quadrature spectrum, where $Q_{xy}(n) = -2\mathrm{Im}\varphi_{xy}(n)$ (i.e. $\mathrm{Im}Q_{xy}(n)$ is the imaginary part of $\varphi_{xy}(n)$).

It is interesting to note that $Q_{xy}(n)$ is negative when a positive value of $x(t)$ is followed a quarter of a cycle later by a negative value of $y(t)$. By way of example if one were measuring, as before, u' and w' in the atmosphere, the sign of $Q_{xy}(n)$ enables one to determine, on average, over which frequency bands (if any) one is systematically making measurements in the upper or lower half of revolving eddies.[3]

When we are dealing with a single signal, $x(t)$ say, the cross-correlations are replaced by autocorrelations (i.e. the average of the products between points a distance τ apart). $S_{xy}(n)$ is replaced by $S_x(n)$ which measures the frequency contributions to the variance of $x(t)$ and is called the power spectrum.

By substituting equations (2) and (4) into (6) we can show that

$$\sigma_{xy}(\tau) = \sum_{k=-\infty}^{\infty} D_k C_k \exp{(2\pi i k\tau/T)}. \qquad \dots (9)$$

Letting $n = k\Delta n$ and $\Delta n = 1/T$ (where k is an integer) the summation version of (7) compared with (9) enables us to write

$$S_{xy}(k\Delta n) = \frac{T}{2}(a_k c_k + b_k d_k) \qquad \dots (10)$$

$$Q_{xy}(k\Delta n) = -\frac{T}{2}(a_k d_k - b_k c_k) \qquad \dots (11)$$

and $S_x(k\Delta n) = \dfrac{T}{2}(a^2_k + b^2_k).$ $\qquad \dots (12)$

Much of this analysis can be found in Hsu[4] and some also in Brooks and Carruthers.[5]

This presents a practical scheme for calculating spectra provided that the Fourier coefficients can be found easily.

The cosine-transform method of producing spectra. Until quite recent times (1965)[6] the labour of producing Fourier coefficients for the utilization of equations (10), (11) and (12) in the production of broad-frequency spectra was considered prohibitive and alternative methods were sought. Apart from electronic and physical wave analysers the most popular mathematical technique was the so-called cosine-transform method. We can show in outline what this involves by taking the Fourier transforms of equation (7) which gives

$$\varphi_{xy}(n) = \int\limits_{-\infty}^{\infty} \varphi_{xy}(\tau)\,\exp\,(-2\pi i n\tau)\,d\tau. \qquad \ldots (13)$$

The cross-correlation is split into odd and even parts $O(\tau)$ and $E(\tau)$

$$\sigma_{xy}(\tau) = \tfrac{1}{2}[\sigma_{xy}(\tau) - \sigma_{xy}(-\tau)] + \tfrac{1}{2}[\sigma_{xy}(\tau) + \sigma_{xy}(-\tau)] = O(\tau) + E(\tau). \qquad \ldots (14)$$

Using this and expanding (13) gives

$$S_{xy}(n) = 4\int\limits_{0}^{\infty} E(\tau)\cos\,2\pi n\tau d\tau, \qquad \ldots (15)$$

and for convenience we also set

$$Q_{xy}(n) = 4\int\limits_{0}^{\infty} O(\tau)\sin\,2\pi n\tau d\tau. \qquad \ldots (16)$$

When $x=y$, $E(\tau)$ becomes the autocorrelation and $S_{xy}(n)$ becomes $S_x(n)$, i.e. the power spectrum.

Letting $n=k/2g\Delta t$, $\tau=L\Delta t$ so that $\delta n=1/2g\Delta t$, the summation version of (15) for $x=y$ becomes

$$\delta n S_x\,(k/2g\Delta t) = \frac{2}{g}\sum_{L=0}^{g}\sigma_x\,(L\Delta t)\cos\frac{\pi k L}{g} \qquad \ldots (17)$$

This provides a scheme of calculation and gives $(g+1)$ spectral estimates at frequencies 0, $1/2g\Delta t$, ..., $1/2\Delta t$ where $1/2\Delta t$ is called the Nyquist frequency which is the maximum usefully analysable frequency for the given data sampling rate $1/\Delta t$. Equation (17) also smooths the results to some extent, and is in fact equivalent to a band-pass filter centred at $k/2g\Delta t$, but having

rather large 'side-lobes' outside the bandwidth δn. (This means that adjacent frequencies interfere with one another.) Further smoothing is therefore necessary. Several functions have been derived which minimize the effect of these 'side-lobes' — one such is called 'hanning' which can be written as

$$S'_k = \tfrac{1}{4}(S_{k-1} + 2S_k + S_{k+1}) \qquad \qquad \ldots (18)$$

so that the terms S'_k form the final spectral estimates. For the practical purposes of estimating the statistical accuracy it is assumed that the spectral values in each frequency band come individually from a multiple of the χ^2 distribution. This being the case the percentage confidence limits applicable to an estimate depend solely on the number of degrees of freedom, ν. In the cosine-transform method $\nu \approx 2N/g$. This arises from the fact that each of the g spectral points effectively averages over the maximum number of possible spectral points (i.e. N/g) in the interval δn and to each of these primitive points are assigned two degrees of freedom corresponding for example to an a_k and b_k or an amplitude and phase. As an example suppose that we require the 90 per cent confidence limits to be roughly 60 per cent and 150 per cent of the value calculated; ν needs to be about 30 and g (the number of lags) must be at the most $N/15$. Inevitably the choice of the number of lags is a compromise between frequency resolution and statistical stability. Several practical details of the cosine-transform method have been omitted and the reader should consult Blackman and Tukey,[7] and Jones[8] for more information. We shall now call the cosine-transform method the B&T method since these authors are generally referred to in the literature.

Concerning the number of arithmetic operations in the B&T method, which we shall need later for a comparison, let an addition $(+)$ and a multiplication $(\times)$ each be for convenience half an operation. Then the computation of the autocorrelations requires

$$N + (N-1) + \ldots + (N-g) = (g+1)(N - g/2) \qquad \ldots (19)$$

full (i.e. $(+\times)$) operations. To evaluate the cosine part of each of the $(g-1)$ spectral points (i.e. ignoring the end points) requires a further $g(+\times)$ operations, i.e. to compute all the spectral points, including end points, requires roughly g^2 operations. Smoothing, for example 'hanning', uses $2(+\times)$ operations for each point. Overall then the total number of operations to produce one power spectrum is about

$$(g+1)(N-g/2) + g^2 + 2g \approx N(1+g) + g^2/2. \qquad \ldots (20)$$

To find cospectra and quadrature spectra from two series of data, $(g+1)(N-g/2)$ operations are required to evaluate the cross-correlations, g additions (i.e. $g/2\,(+\times)$ operations) are wanted to form $E(\tau)$ and $O(\tau)$, there are then $2g^2$ operations to form the cosine and sine transforms plus finally $4g$ smoothing operations, i.e. altogether

$$(g+1)(N-g/2) + g/2 + 2g^2 + 4g \approx N(1+g) + 3g^2/2 \qquad \ldots (21)$$

operations.

The Fast Fourier Transform (FFT). For a discrete, equally spaced time series, of zero mean, where t = time (this could instead be a space

variable), $N=$the number of data points and $n=$a frequency, writing $t=j\Delta t$, $(j=0, 1, \ldots, N-1)$, $T=N\Delta t$ and $n=k/T=k\Delta n$, $(k=0, 1, \ldots, N-1)$, ignoring end corrections the summation version of equation (3) is :

$$C\,(k\Delta n) = \frac{1}{N} \sum_{j=0}^{N-1} x\,(j\Delta t)\; W^{jk} \qquad \ldots (22)$$

where $W=\exp(2\pi i/N)$ and C_k is replaced by $C(k\Delta n)$ to indicate that the Fourier coefficients are evaluated at frequency intervals Δn starting at zero frequency. Only about $N/2$ useful coefficients are produced by (22), the rest being a set of reflected values, and straightforward (i.e. classical) calculation requires about $N^2/2$ $(+\times)$ operations (i.e. each of the N data points has to be multiplied by a trigonometric function to obtain each of the $N/2$ coefficients). In 1965 Cooley and Tukey[6] produced a paper which showed that the number of operations could be reduced to about $2N\log_2 N$ with no loss of information and in fact with increased computational accuracy. By sorting the data this number can be reduced even further to about $N\log_2 N$. The FFT works fastest when $N=3^m$, where m is an integer, but normally factors 2^m and 4^m are used, and for 1024 points the speed of computation can be increased by about 50 times (i.e. $(1024)^2/2(1024\times10)=51\cdot2$). In addition the FFT can ideally be adapted for computer evaluations.

The basis of the FFT is that a large number of the W^{jk} terms are equal, or the negative of each other, so that if the data points (i.e. $x(t)$) which are multiplied by the same term are brought together first a vast saving in arithmetic results. To illustrate this in a simple case let $N=4$ so that immediate evaluation of (22) (ignoring the $1/N$) produces

$C(0)=x(0)+x(1)+x(2)+x(3)$
$C(1)=x(0)+x(1)W^1+x(2)W^2+x(3)W^3$
$C(2)=x(0)+x(1)W^2+x(2)W^4+x(3)W^6$
$C(3)=x(0)+x(1)W^3+x(2)W^6+x(3)W^9.$

Now $W^1=i$, $W^2=-1$, $W^3=-i$, $W^4=1$, and the cycle then repeats with $W^5=i$, $W^6=-1$ etc., so that if we let

$X(0)=x(0)+x(2)$, $X(1)=x(0)-x(2)$, $X(2)=x(1)+x(3)$,
and $X(3)=x(1)-x(3)$,

we then have

$C(0)=X(0)+X(2)$
$C(1)=X(1)+X(3)W^1$
$C(2)=X(0)+X(2)W^2$
$C(3)=X(1)+X(3)W^3.$

The number of steps is thereby cut down from 12 additions and 9 multiplications to 8 additions and 3 multiplications.

A discussion of the theory behind the FFT together with results, references and KDF 9 USER CODE programmes is given by Rayment.[9]

To find spectra therefore the Fourier coefficients are substituted directly into equations (10), (11) and (12). The spectral points will in general require more smoothing than the spectra derived using the B&T method. Probably one or two applications of the previously mentioned 'hanning' formula

together with linear averaging over adjacent points will normally suffice. The same statistical arguments apply to these estimates and the number of degrees of freedom to be attached to each final point is $2H$ where H is the number of adjacent points averaged together.

Concerning the number of $(+\times)$ operations we require $N\log_2 N$ to produce the coefficients, $3N/4$ for the power spectrum points and $2N+(1+1/H)\,N/4$ for a double application of hanning and linear averaging. Computation of the variance, i.e. the area under the spectral curve, which is given automatically in the B&T method, requires $N/2$ additions, i.e. $N/4$ $(+\times)$ operations. Cospectra together with quadrature spectra simply need double the number of operations that are required to find the power spectra. The overall number of operations per spectrum is therefore

$$N(\log_2 N + 3\cdot25 + 1/4H). \qquad \dots (23)$$

It should be mentioned that there is a further reduction in the number of degrees of freedom, in both the B&T method and the FFT, connected with end effects which we shall ignore here.[7,10] Also it is possible in both methods to increase stability by averaging over several spectral curves if conditions permit this.

Without discussing any details it may be of interest to list some other applications of the FFT.

(i)   Computation of Fourier integrals, Fourier series, convolution integrals, computing difference equations and simulating filters (Ref. 10).

(ii) Trigonometric interpolation, least-squares approximation by trigonometric polynomials, numerical convolution and digital filtering (Ref. 11).

(iii) Calculating high-order correlations (Ref. 12).

Comparison between the FFT and the B&T method. For the sake of a comparison between the two methods we shall take a case where $N=1024$ and $v=30$, i.e. $g=N/15$ and $H=15$. To produce power spectra and the variance together with the suggested smoothing techniques requires for the B&T method, substituting in the right-hand side of equation (20),

$$1024(1+1024/15)+\tfrac{1}{2}(1024/15)^2=73\ 259 \text{ operations,}$$

and the FFT requires, referring to equation (23),

$$1024(10+3\cdot25+1/60)=13\ 585 \text{ operations.}$$

The ratio of the numbers of operations is $5\cdot39$ so that the FFT is much more efficient.

In this example however if one can accept a coarser frequency resolution such that $g=12$ (i.e. $H=85$ and $v=170$) the numbers of operations work out to be nearly equal. The general expression for the number of operations to be equal is :

$$2N/g=2H=v\approx\left\{N+\sqrt{[N^2+2N(2\cdot25+\log_2 N)]}\right\}/(2\cdot25+\log_2 N). \quad \dots (24)$$

(In the example we are using therefore $g=12\cdot18$ gives exact equivalence though in practice g must be a whole number.) So that if we can accept $g\leqslant12$, for $N=1024$, the B&T method of producing power spectra is preferable.
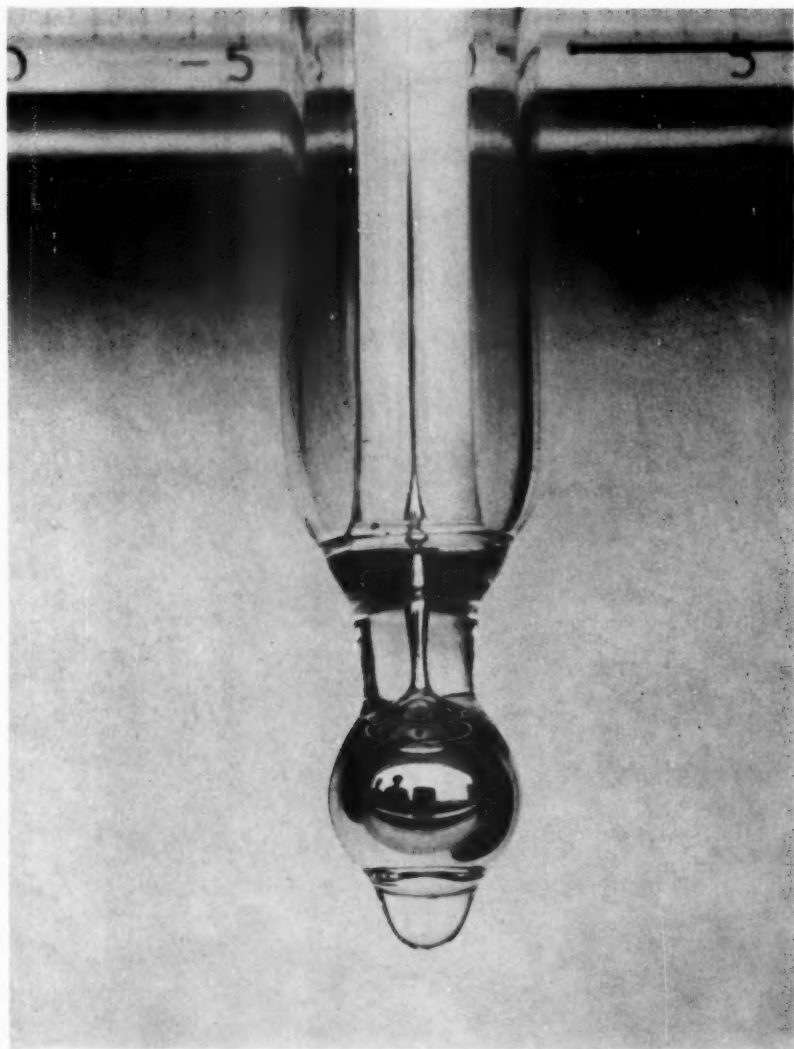
PLATE I—THE SPECIAL DRY-BULB THERMOMETER AT RAE, BEDFORD

Moisture which had accumulated during the wet fog of 28 May 1968 had coalesced and run down the thermometer stem, forming an unstable drop some 3·5 mm long on the underside of the thermometer bulb. See page 275.
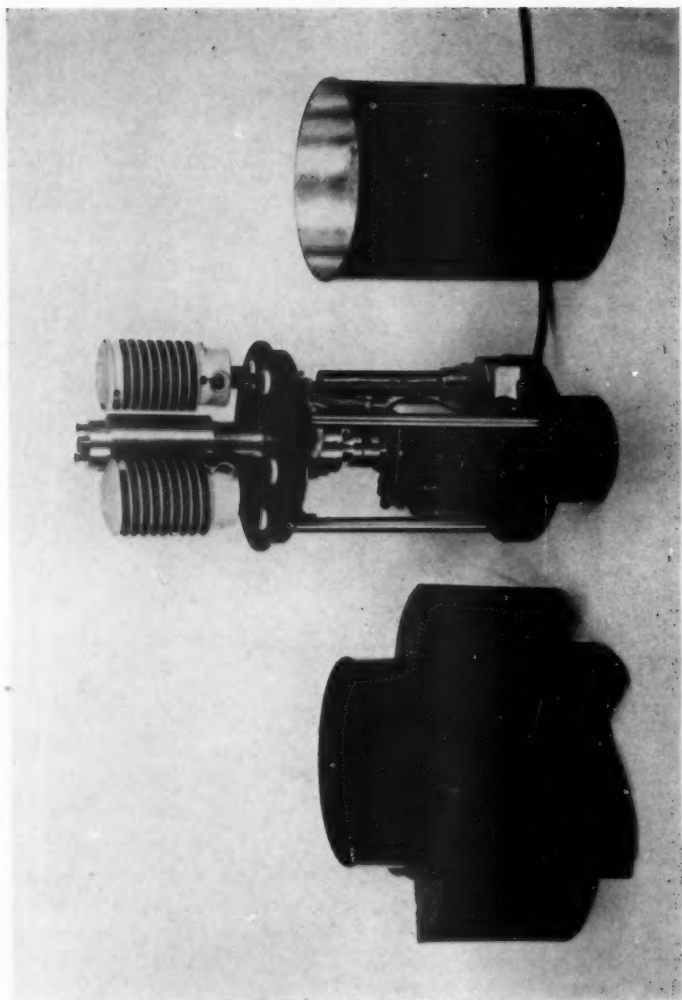
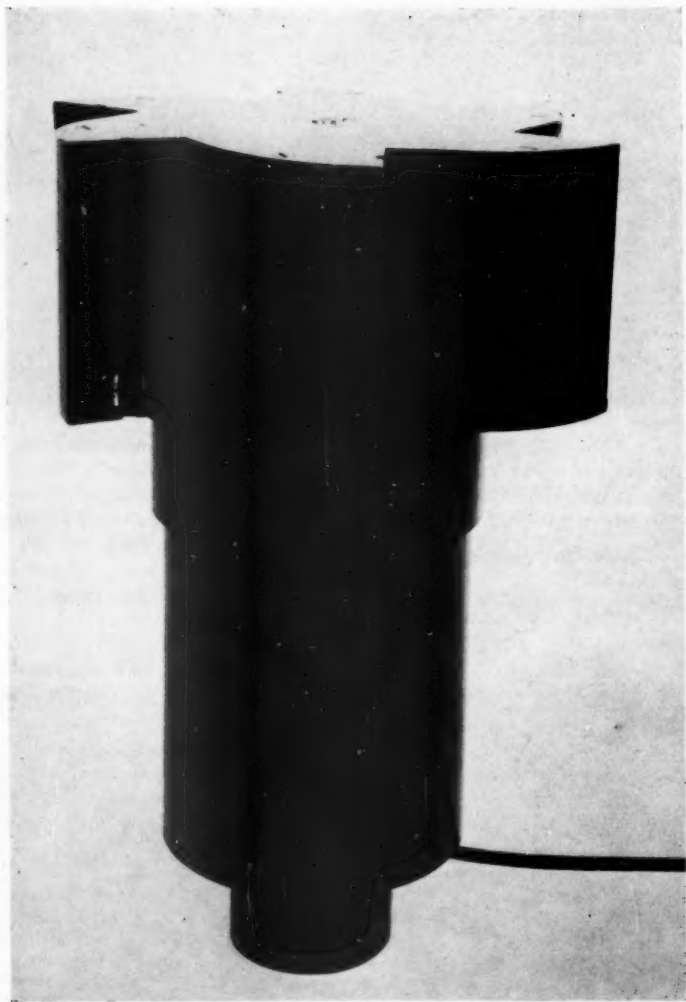PLATE II—COMPONENT PARTS OF HEATED ANEMOMETER
See page 270.

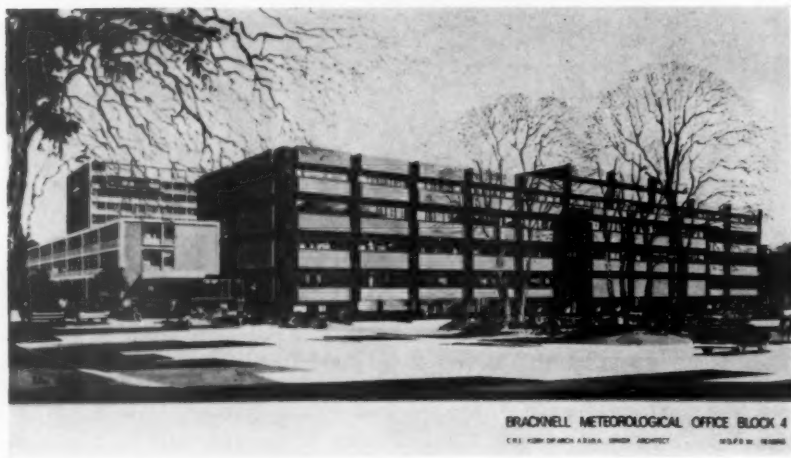PLATE III—HEATED ANEMOMETER ASSEMBLED
See page 270.

PLATE IV—SHALLOW FOG OVER A SNOW SURFACE

The photograph was taken at about 0915 GMT on 15 February 1970 from 300 yd north-north-west of the Control Tower on the airfield at Machrihanish, Argyll, with the camera facing south-south-east. (See page 284.)

PLATE V—ARTIST'S IMPRESSION OF THE RICHARDSON WING NOW UNDER CONSTRUCTION AT HEADQUARTERS, METEOROLOGICAL OFFICE, BRACKNELL

Going back to the example where $g = N/15$, but where we have two series of data points each of number N, the situation for the production of cospectra and quadrature spectra favours the B&T method slightly more, compared with the FFT, than it did in the power spectrum case. To produce these spectra therefore plus the covariance but not the area under the quadrature spectrum curve requires for the FFT twice the figure for the power spectrum case minus the $N/4$ operations required to find the area, i.e. 26 914 operations. For the B&T method, substituting into equation (21), the number of operations is

$$1024(1 + 1024/15) + \frac{3}{2}(1024/15)^2 = 77\ 920.$$

This gives the ratio of the numbers of operations as 2·89.

If all the spectra are required (i.e. cospectrum plus covariance, quadrature spectrum and both power spectra plus the variances) the FFT gains tremendously because the same Fourier coefficients can be used for the power spectra and the cospectra and quadrature spectra whereas the B&T method requires a fresh set of cross-products each time (i.e. three sets altogether, one for each of the power spectra and one set for the cospectra and quadrature spectra). For the FFT therefore the number of operations is twice that for the power spectrum case plus the previously found number for the cospectra and quadrature spectra minus the number of operations to produce two sets of Fourier coefficients (i.e. $-2N\log_2 N$), i.e. $(2 \times 13\ 585) + 26\ 914 - (2 \times 1024 \times 10) = 33\ 604$. For the B&T method we require twice that for the power spectrum case plus that for the cospectra and quadrature spectra, i.e. $(2 \times 73\ 259) + 77\ 920 = 224\ 438$ operations, giving a ratio of operations in favour of the FFT equal to 6·68.

Conclusions. The requirement for a small amount of spectral information, with low-frequency resolution, can still be met by the B&T method but it is clear that in many situations use of the FFT can drastically reduce the computational time thereby allowing some problems to be tackled which hitherto could only be solved in a very rough way, if attempted at all. The FFT enables one to perform extensive analysis, if required, not only of spectra and cospectra but also of higher-order spectra (polyspectra) with the maximum possible frequency resolution and computational accuracy.

REFERENCES

1. WIENER, N.; The Fourier integral. Cambridge, Cambridge University Press, 1933.
2. TAYLOR, G. I.; The spectrum of turbulence. *Proc. R. Soc., London, A*, **164**, 1938, pp. 476–490.
3. LUMLEY, J. L. and PANOFSKY, H. A.; The structure of atmospheric turbulence. Interscience Monographs and Texts in Physics and Astronomy, Vol. XII. New York, London and Sydney, John Wiley and Sons, 1964.
4. HSU, H. P.; Outline of Fourier analysis. London, Iliffe Books Ltd, 1967.
5. BROOKS, C. E. P. and CARRUTHERS, N.; Handbook of statistical methods in meteorology. London, HMSO, 1953.
6. COOLEY, J. W. and TUKEY, J. W.; An algorithm for the machine calculation of complex Fourier series. *Maths Comput., Providence, R.I.*, **19**, 1965, pp. 297–301.

7. BLACKMAN, R. B. and TUKEY, J. W.; The measurement of power spectra. New York, Dover, 1958.
8. JONES, R. A.; Studies of eddy structure in the first few thousand feet of the atmosphere. London, Meteorological Office, Part 2 1957 and Part 3 1958. Unpublished, available in Meteorological Office Library, Bracknell.
9. RAYMENT, R.; Spectral analysis using the Fast Fourier Transform. London, Meteorological Office, 1970. Unpublished, available in Meteorological Office Library, Bracknell.
10. New York, Institute of Radio Engineers. *I.R.E. Transactions on Audio and Electroacoustics*, AU15, 1967, No. 2.
11. GENTLEMAN, W. M. and SANDE, G.; Fast Fourier Transforms for fun and profit. American Federation of Information Processing Societies. Proceedings of the Fall Joint Computer Conference, Washington, 1966.
12. VAN ATTA, C. W. and CHEN, W. Y.; Correlation measurements in grid turbulence using digital harmonic analysis. *Jnl fluid Mech.*, *London*, **34**, 1968, pp. 497–515.

A HEATED ANEMOMETER

By G. E. W. HARTLEY

Summary. Some details and drawings are given for a heated anemometer designed by the Meteorological Office and installed on Mount Olympus, Greece in early 1969.

A rotor is arranged so that its six cups have their interior surfaces exposed to two 600-watt bowl-fire elements connected to a 240-volt a.c. supply and controlled by a thermostat set at 36°F. A direct-current generator is driven by the spindle of the rotor and operates a Mk 2 anemometer wind-speed dial adapted for direct current and marked for wind speeds up to 150 knots.

Calibration was done in two stages. A relation was obtained between wind speed and rotor revolutions per minute from 5 to 90 knots in a wind-tunnel and the calibration graph was extrapolated to 150 knots. The generator was then driven at various speeds in the range to calibrate the dial up to speeds of 150 knots.

D. W. Mann and C. F. Marvin* have described a heated rotation anemometer designed and made for use on Mount Washington, U.S.A., and when the Meteorological Office proposed to produce a heated anemometer for use on Mount Olympus, Greece, at a height of about 6000 feet (approximately 1800 metres), this anemometer was considered to be the most hopeful design.

The first attempt, which was not successful, was to use a standard Mk 2 cup-generator anemometer, the cups being replaced by a six-cup rotor on the lines of that of the Mount Washington anemometer, and to heat the rotor by means of a 'Thermo-Cord' heating wire, of the kind used to prevent pipes from freezing, wound round a cylinder inside the rotor, the cylinder being held on a circular plate fixed to the generator housing, with a very small clearance between the rim of the plate and the rotor, so as to prevent snow or rain blowing into the rotor.

The rotor consisted of six cups fixed to the outside wall of a cylinder closed at the upper end, the heating coil being as close as possible to the inside of the cylinder. This arrangement was unsuccessful because not enough heat reached the cups through the cylinder wall to melt snow which collected in the cups. Also the torque produced by this rotor was considerably less than that produced by the standard cup assembly, and so the starting speed was about 10 knots; the calibration also differed from that of the standard cups, so that the dial had to be altered.

---

* *Mon. Weath. Rev. U.S. Dep. Agric., Washington DC*, **6a**, 1934, pp. 189–193 (from 'The great wind of April 11–12, 1934 on Mount Washington, N.H. and its measurement' parts II and III).

A second heated anemometer was therefore designed; it is illustrated in Plates II and III, and in Figures 1 and 2. Part numbers in the descriptions refer to part numbers in Figure 1.
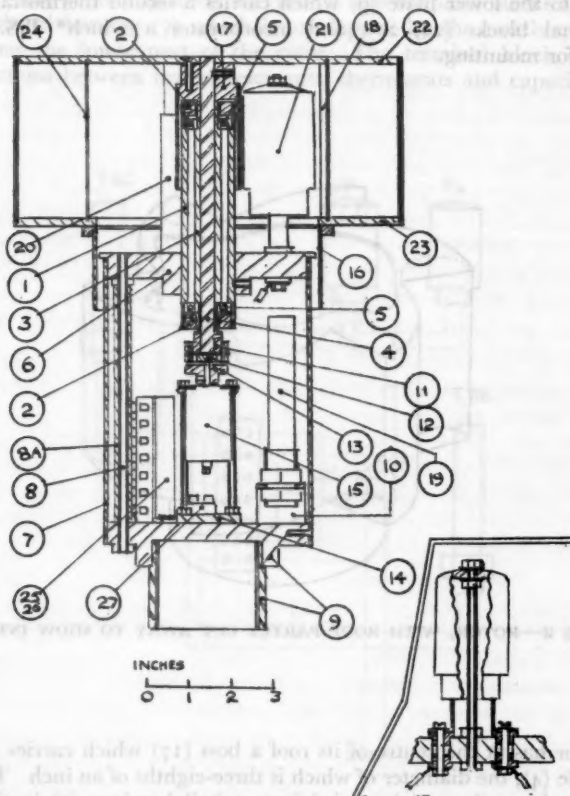

FIGURE 1—GENERAL ARRANGEMENT OF HEATED ANEMOMETER INCLUDING INSET SHOWING STRENGTHENED MOUNTING OF HEATING ELEMENT

List of part numbers and description of parts :

1. Spindle bearing support tube.	11, 12, 13. Flexible coupling.
2. Ball bearing retaining cups (2).	14. Generator mount.
3. Spindle outer sleeve.	15. Generator.
4. Spindle.	16. Rotor skirt (or weather shield).
5. Ball bearings (2) 1⅛″ external dia-	17. Rotor boss.
meter × ⅜″ internal diameter × ⅜″ thick.	18, 22, 23, 24. Parts of rotor.
6. Upper plate.	19. Lower thermostat.
7. Housing.	20. Upper thermostat.
8, 8A. Pillars (3).	21. Heating elements (2).
9. Lower plate and mounting socket.	25, 26, 27. Terminal blocks and bracket.
10. Lower thermostat bracket.	

The rotor, shown in isometric view in Figure 2, is arranged so that its six 'cups' have their interior surfaces exposed to the heating elements (21). These are two 600-watt bowl-fire elements, strap-mounted in a vertical position on the circular plate (6) which also carries the rotor spindle bearing support tube (1) and a thermostat (20). Pillars (8, 8A) on the underside of plate (6) connect it to the lower plate (9) which carries a second thermostat (19) and two terminal blocks (26, 27), and incorporates a 2-inch* B.S.P. tapped socket (9) for mounting.
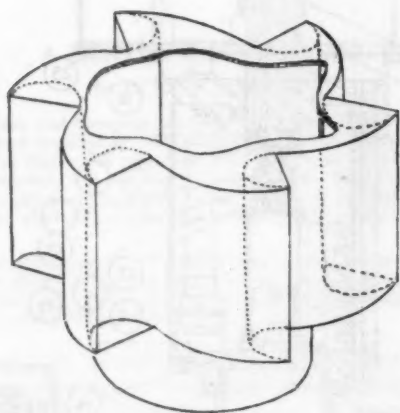
FIGURE 2—ROTOR, WITH ROOF PARTLY CUT AWAY TO SHOW INTERIOR

The rotor has at the centre of its roof a boss (17) which carries a stainless-steel spindle (4), the diameter of which is three-eighths of an inch. The spindle fits inside a brass sleeve (3) carried in two ball bearings (2) in the bearing support tube (1). The rotor and spindle can be lifted out of the sleeve, leaving the sleeve and bearings in position, after taking off the upper generator coupling piece (11).

The generator (15) driven by the spindle through the flexible coupling (11, 12, 13) is a 'Servo-Tek' tachometer generator, type SA 740A-2, giving 7·0 volts d.c. per 1000 rev/min with a driving torque not exceeding 0·20 in ozf. This was chosen because of its small size, low driving torque and the claim by its makers of long brush and bearing life. Its connecting leads are taken out to the terminal block (27). The two heating elements are connected in parallel across the 240-V a.c. supply, one of the connecting leads being

* Dimensions are given in British units because, at the time of making, metric equipment and materials were not readily available.

connected through the two cartridge-type thermostats which are in series. The lower thermostat (19) is set to close at 36°F, and the upper (20) to open at 60°F, to act as a safety device to prevent the rotor getting too hot in case the 36° thermostat fails to open. The thermostat contacts have 0·05 mF (700-V rating) capacitors connected across them to prevent sparking (see Figure 3). The generator, lower thermostat and terminal blocks are enclosed in a cylindrical housing (7) which is overlapped by the weather shield (16) which forms the lower part of the rotor. The terminal block (26) makes the connections between heating elements, thermostats and capacitors easier.
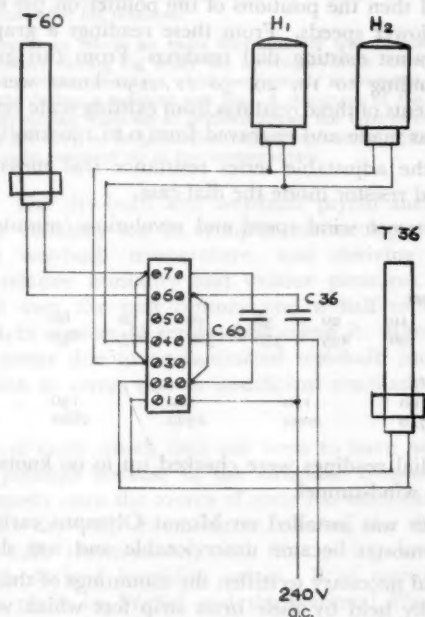

FIGURE 3—HEATING CIRCUIT WIRING DIAGRAM

T_{60}, T_{36} Thermostats; C_{60}, C_{36} Capacitors; H_1, H_2 Heating elements.

The anemometer was only required to operate one dial, and a standard wind-speed dial as used with Mk 2 and Mk 4 anemometers was adapted to direct current by taking out the rectifier, and adjusting the series resistance as required. The anemometer was calibrated first with a worm reduction gear, with a pointer on the worm-wheel spindle, in place of the generator, to obtain a relation between wind speed and rotor rev/min. This was done in the large wind-tunnel at the Meteorological Office, Bracknell, from starting speed up to 90 knots, and the calibration graph was extrapolated up to 150 knots. This means of course that above 90 knots readings are suspect; but the method was the only possible one with the existing wind-tunnel.

The relation between wind speed and rev/min having been obtained, it was required to drive the generator at various speeds in the range, to calibrate the dial. This was done by fitting the generator with a small wind-mill fan, whose spindle also carried a worm reduction gear and pointer, so that revolutions could be counted against a stop-watch. The fan, generator and counter were mounted in the small wind-tunnel, as a means of driving the fan and hence the generator, at speeds up to that corresponding to 150 knots, though of course the wind speed in the small tunnel was not measured.

The generator was connected to the modified dial with an adjustable series resistance. At a speed corresponding to 150 knots, the series resistance was adjusted to make the dial read full-scale deflexion (90 knots on the existing scale) and then the positions of the pointer on the existing scale were noted at various lower speeds. From these readings a graph was drawn up of wind speed against existing dial readings From this graph existing dial readings corresponding to 10, 20, 30 ... 150 knots were obtained. The angular displacements of these readings from existing scale zero were measured, and a new dial was made and engraved from 0 to 150 knots.

The value of the adjustable series resistance was measured, and it was replaced by a fixed resistor inside the dial case.

The relation between wind speed and revolutions/minute is shown in the following table:

Experimental values

knots	5	10	20	30	40	50	60	70	80	90
rev/min	13	96	235	370	520	675	840	1040	1235	1480

Extrapolated values

knots	100	110	120	130	140	150
rev/min	1740	2020	2320	2620	2950	3300

The engraved dial readings were checked up to 90 knots with the anemometer in the large wind-tunnel.

The anemometer was installed on Mount Olympus early in 1969. Fairly soon the 60° thermostat became unserviceable and was short-circuited out.

It was also found necessary to stiffen the mountings of the heating elements, which were initially held by their brass strip feet which were bolted to the plate (6) with insulating sleeves interposed, the bolts forming the electrical connections. To stiffen the mountings, ¼-inch steel screwed rod held by two nuts in a ¼-inch diameter hole midway between the feet was passed up through the central hole of the ceramic former of the heating element, with a locknut above and below the top of the former, and of such a length that the top of the screwed rod was clear of the roof of the rotor — see inset in Figure 1.

Latest reports from Mount Olympus (spring 1970) suggest that the anemometer is now satisfactory, and that it is questionable whether the 60°F thermostat is necessary.

THE EFFECT OF A MOISTURE-COVERED DRY-BULB THERMOMETER ON AIR TEMPERATURE READINGS AND THE DERIVED HUMIDITY VALUES

By D. J. GEORGE

Summary. In certain circumstances moisture may be deposited on the bulb of the dry-bulb thermometer in a standard screen. A photograph is shown of a drop of water which formed on a bulb during a summer wet fog. The moisture-covered thermometer may read up to 1 degC too low during the evaporation stage until all the moisture has evaporated which may not be until several hours after fog dispersal.

Experiments were made in which an extra thermometer was installed in the screen, and allowed to collect moisture during fog while the screen dry-bulb thermometer was kept dry by wiping with a cloth between readings which were made at frequent intervals. Details are given of readings made during a summer wet fog. A summary of the results for 7 summer fogs and 11 winter fogs during 1968–69 at Bedford shows the type of error which can occur. It is shown that errors are likely to be greatest at high temperatures with dry air and moderate winds and least with moist stagnant air at low temperatures.

Introduction. The dry-bulb and wet-bulb psychrometer in a standard screen is in fairly common use in synoptic meteorology for measuring air temperature and wet-bulb temperature, and deriving humidity values (e.g. dew-point, relative humidity and vapour pressure). Much attention has been devoted over the past century and a half to the theory of the psychrometer and to sources of error when using it. Recently, McCaffery[1] has investigated errors due to contaminated wet-bulb muslins, and Zobel[2] has drawn attention to errors due to insufficient ventilation of the wet-bulb thermometer.

Another source of error which does not seem to have had much attention in meteorology (perhaps because of the irregular frequency of occurrence and the simple remedy once the source of error has been detected) is moisture on the bulb of the dry-bulb thermometer, causing the thermometer to act as a partial wet-bulb thermometer, and thus giving low air temperature readings and high derived humidity values. Brief mention of this source of error has been made by Wylie[3] and the National Physical Laboratory.[4] Standard textbooks on observing[5] and meteorological instruments[6] instruct the observer to keep thermometers clean and bright, without defining situations where the observer should be especially watchful for the presence of moisture on the thermometers.

The purpose of this note is to draw attention to the magnitude and persistence of errors in dry-bulb temperature and the derived humidity values, caused by using readings from a moisture-covered mercury-in-glass dry-bulb thermometer in a standard screen, by means of examples observed during 1968–69 at the Royal Aircraft Establishment, Bedford (altitude 85 m). Errors of almost 1 degC in dry-bulb temperature and dew-point, 10 per cent in relative humidity and 0·8 mb in vapour pressure were observed several hours after fog dispersal. Knowledge of situations when moisture is likely to form on thermometers may enable observers to take prompt remedial action and thus obtain more accurate values.

Formation and evaporation of moisture. Moisture commonly forms on all surfaces inside and outside the screen by condensation of water vapour during water fog or hill fog, and may be augmented in hill fog by fog droplets blowing into the screen. Observations show that during water fog a mist forms on the screen thermometers in about 45 to 90 minutes, and in about 10 minutes in wet fog or hill fog. Small droplets coalesce and gravitate to form a drop on the underside of the thermometer bulb after several hours of accumulation (see Plate I). For a spherical bulb of diameter 1 cm, the limiting size of drop is about 4 mm. After growing to this size the drop falls off (particularly if the screen is vibrated) and growth starts afresh. A thin layer of ice grows on the thermometers by deposition of water vapour during supercooled water fog.

Evaporation of the drop commences when the visibility improves from thick fog conditions to over 1 km. The moisture-covered thermometer reads low during the evaporation stage until all the moisture has evaporated.

Errors in air temperature and the derived humidity values. The error ΔT in the dry-bulb temperature due to taking readings from a moisture-covered dry-bulb thermometer (T') instead of a perfectly dry dry-bulb thermometer (T) will be proportional to the wet-bulb depression, itself a function of the general temperature level and the rate of evaporation.

Any error in the dry-bulb temperature will be reflected in a reduced wet-bulb depression and in turn will produce errors in the derived humidity values. By combining the hygrometric equation[7] with an expression for relative humidity in terms of vapour pressure, equations may be obtained showing the error in relative humidity ΔU :

$$\Delta U = 100 \; \frac{e_{s(Tw)} - Ap\,(T' - T_w)}{e_{s(T')}} - 100 \; \frac{e_{s\,(Tw)} - Ap(T - T_w)}{e_{s\,(T)}} \quad \dots (1)$$

$$\approx \frac{100\;Ap}{e_{s(T)}}\,\Delta T$$

where $e_{s(Tw)}$ = saturation vapour pressure at the wet-bulb temperature Tw
$\quad\;\; e_{s(T)}$ = saturation vapour pressure at the dry-bulb temperature T
$\quad\;\; Ap$ = psychrometric constant.

By similarly applying the hygrometric equation it can be shown that the error in vapour pressure Δe is proportional to ΔT. Also, as the dew-point by definition is the temperature at which $e = e_s$, errors in dew-point ΔD will also be proportional to ΔT.

Errors in measured air temperature and the derived humidity values are thus likely to be greatest at high temperatures ($> 10°C$) with dry air and moderate winds, and least with moist stagnant air or at low temperatures.

Spencer-Gregory and Rourke[8] give equations which show that the rate of evaporation of a given mass of water from a thermometer bulb is proportional to the wet-bulb depression and square root of the wind speed. The longest time for a drop to evaporate from a moisture-covered bulb will occur when there is a large drop after prolonged or wet fog, followed by light winds and high relative humidity (e.g. after fog dispersal in summer with cloudy skies and slow temperature rise, or in winter). A drop will evaporate relatively quickly in summer with moderate winds, clear skies and rapidly decreasing relative humidity.

Experiments. Comparative experiments were made by installing a second dry-bulb thermometer (known as the special dry-bulb thermometer) to the right of the screen dry-bulb thermometer, and allowing the special thermometer to collect moisture during fog. The moisture was allowed to evaporate naturally, while the screen dry-bulb thermometer was kept dry by wiping it with a clean cloth between readings. Frequent readings of temperatures and supporting observations were made during and after the fog until all the moisture had evaporated.

A typical example of summer wet fog occurred on 28 May 1968 when there was a north-east airflow over the Midlands and East Anglia. Fog formed soon after midnight when moist air from the Wash had cooled over-land, producing wet fog with visibility < 90 m and light north-east wind until o8 GMT, all objects being dripping wet. The fog thinned after o8 GMT, with mist and low cloud during the morning and broken cumulus in the afternoon. Moisture formed on the special thermometer by 0115 and by 0958 it had grown to a drop some 3 to 4 mm long (see Plate I). The readings and errors are shown in Figure 1.

Results of other experiments are summarized in Table I. The heaviest condensation occurred with pure water fogs with very low visibility during the life of the fogs, while short-lived fogs, shallow fogs with variable visibility and fogs with smoke content, produced little condensation.

Experiments continued with 11 fogs during the winter of 1968–69. Although much moisture accumulated during prolonged fogs at temperatures between − 2 and + 10°C, evaporation generally took place slowly, and errors in dry-bulb temperature averaged 0·1 degC, with a maximum error of 0·2 degC.

Another experiment showed that it is possible for melting snowflakes to adhere to the thermometer bulb after being blown into the screen during snow showers, and that errors in air temperature readings and derived humidity values can occur while the snowflakes melt and evaporate.

Discussion. It is apparent from these simple experiments that significant errors in measured air temperature and derived humidity values can occur if moisture forming on the dry-bulb thermometer during water fogs at tempera-tures above freezing goes undetected and is allowed to evaporate after fog dispersal. Measured and reported air temperatures and dew-points may be up to 1 degC too low and too high respectively during the evaporation stage. If these erroneous values are used for graphical calculation of convection condensation levels (CCLs) on the tephigram, a too-low assessment of cloud base can be made (e.g. CCLs using the readings at 1242 GMT on 28 May 1968 were 1600 ft using the screen dry-bulb temperature, and 700 ft using the special dry-bulb temperature, the estimated cumulus base being 1500 ft).

Although most observers are well aware of the care required with wet-bulb thermometers, the dry-bulb thermometer tends to be taken for granted. A watch should be kept for moisture on thermometers during and after fog or wintry precipitation, and any deposit on the bulbs of screen thermometers should be wiped off with a clean tissue or cloth.

With increasing use of remote indicating thermometers at synoptic stations and on high masts and mountains, this source of error may become more

TABLE I—SUMMARIZED RESULTS OF EXPERIMENTS WITH SUMMER HALF-YEAR FOGS

Date 1968	Type of fog	Duration of fog	Time from beginning of evaporation of drop, to complete evaporation	Max. ΔT	Mean ΔT	Max. ΔD	Mean ΔD	Max. ΔU	Mean ΔU	Max. Δe	Mean Δe
				degrees	Celsius			for cent		millibars	
10 April	wet advection	4 h 30 min	2 h 22 min	0·7	0·27	0·8	0·35	9	3·9	0·4	0·20
24 May	radiation	5 h 30 min	1 h 15 min	0·5	0·38	0·5	0·40	7	5·2	0·4	0·28
28 May	wet advection/radiation	9 h 20 min	4 h 30 min	0·9	0·44	0·9	0·41	10	4·3	0·8	0·38
22 August	shallow radiation	4 h 40 min	no discernible moisture on bulb	0·0	0·0	0·0	0·0	0	0·0	0·0	0·0
23 August	radiation	8 h 15 min	2 h 25 min bulb slightly misty at 0653 GMT	0·5	0·32	0·4	0·23	5	3·2	0·5	0·28
5 September	radiation	1 h 50 min		0·1	—	0·1	—	1	—	0·1	—
10 September	radiation	8 h 15 min	2 h 40 min	0·4	0·25	0·3	0·18	6	2·6	0·4	0·22
Mean values for 2 advection fogs (10 April and 28 May)				0·80	0·35	0·85	0·38	9·5	4·1	0·60	0·29
Mean values for 3 radiation fogs (24 May, 23 August and 10 Sept.)				0·47	0·32	0·40	0·27	5·3	3·7	0·43	0·26

ΔT Error in dry-bulb temperature
ΔU Error in relative humidity
ΔD Error in dew-point temperature
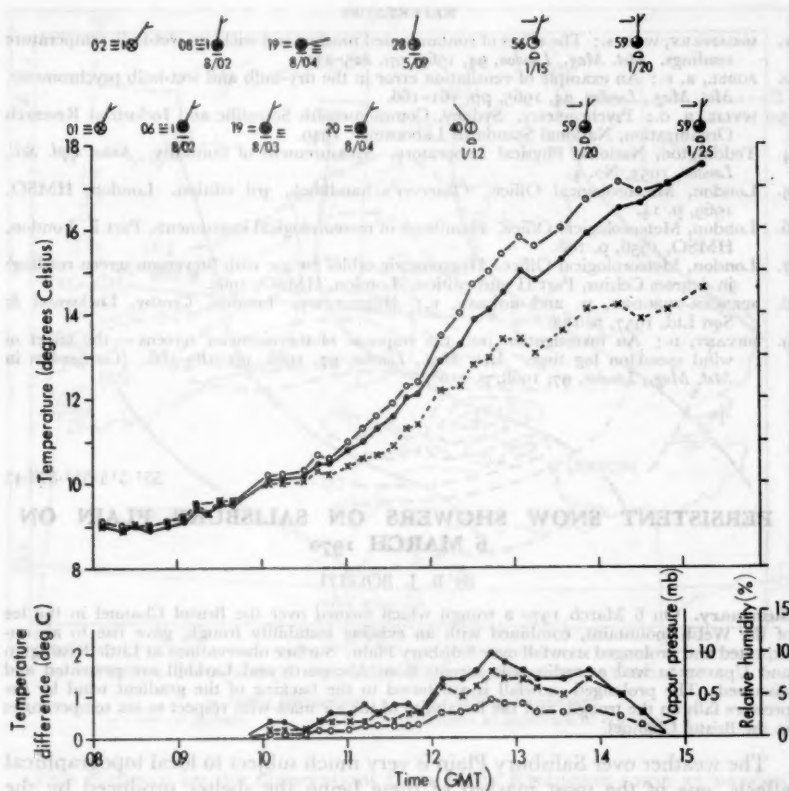Δe Error in vapour pressure

FIGURE I—THE EXPERIMENT AT RAE, BEDFORD, ON 28 MAY 1968
Upper curves — thermometer readings of :
o———o Dry bulb;   .———. Moisture-covered dry bulb;   x – – – x Wet bulb.
Lower curves — errors arising from use of moisture-covered dry-bulb thermometer in :
.———. Relative humidity;   x———x Vapour pressure;   o———o Dew-point tempera-
ture.

important, particularly where the temperature elements are exposed to hill
fog or cloud for long periods, and only visited at infrequent intervals. The
remedy then may be to instal some device for drying off the dry-bulb element
after fog.

These errors may be compounded with errors due to insufficient ventilation
of the thermometers (described by Zobel[2]), or errors due to the lag of the
screen itself (described by Bryant[3]).

REFERENCES

1. MCCAFFERY, W. D. S.; The effect of contaminated muslins and wicks on wet-bulb temperature readings. *Met. Mag., London*, **94**, 1965, pp. 225–231.
2. ZOBEL, R. F.; An example of ventilation error in the dry-bulb and wet-bulb psychrometer. *Met. Mag., London*, **94**, 1965, pp. 161–166.
3. WYLIE, R. G.; Psychrometry. Sydney, Commonwealth Scientific and Industrial Research Organization, National Standards Laboratory, 1949.
4. Teddington, National Physical Laboratory. Measurement of humidity. *Notes appl. Sci., London*, 1953, No. 4.
5. London, Meteorological Office. Observer's handbook, 3rd edition. London, HMSO, 1969, p. 14.
6. London, Meteorological Office. Handbook of meteorological instruments, Part I. London, HMSO, 1956, p. 108.
7. London, Meteorological Office. Hygrometric tables for use with Stevenson screen readings in degrees Celsius, Part II 2nd edition. London, HMSO, 1964.
8. SPENCER-GREGORY, H. and ROURKE, E.; Hygrometry. London, Crosby, Lockwood & Son Ltd, 1957, p. 153.
9. BRYANT, D.; An investigation into the response of thermometer screens — the effect of wind speed on lag time. *Met. Mag., London*, **97**, 1968, pp. 183–186. (*Corrigendum* in *Met. Mag., London*, **97**, 1968, p. 256).

551.515:551.578.45

PERSISTENT SNOW SHOWERS ON SALISBURY PLAIN ON 6 MARCH 1970

By B. J. BOOTH

Summary. On 6 March 1970 a trough which formed over the Bristol Channel in the lee of the Welsh mountains, combined with an existing instability trough, gave rise to an unexpected and prolonged snowfall over Salisbury Plain. Surface observations at Little Rissington and Upavon as well as radiosonde ascents from Aberporth and Larkhill are presented and discussed. The prolonged snowfall is attributed to the backing of the gradient wind by the pressure falls on the trough, and the instability of the air mass with respect to sea temperatures in the Bristol Channel.

The weather over Salisbury Plain is very much subject to local topographical effects, one of the most marked of these being the shelter produced by the Welsh mountains in unstable west-north-westerly – north-north-westerly airstreams during winter. Another effect of the Welsh mountains in north-westerly airstreams is to produce a lee trough over the Bristol Channel. Sometimes the result of this latter is not immediately noticeable, but on 6 March 1970, it helped to produce an unexpected, relatively prolonged snowfall lasting nearly four hours over Salisbury Plain and resulting in nearly half an inch* of snow over the highest ground.

At 06 GMT an unstable north-westerly airflow covered the British Isles. A minor trough lay from Shawbury to Birr in Eire (Figure 1) and was moving south at 15 knots.* Pressure tendencies ahead of the trough were slight, the largest fall being 0·7 mb in 3 hours; further very slight falls were being reported from the Bristol Channel as a lee trough formed. Over southern counties and behind the trough there was a very slight pressure rise. The overall effect was for the gradient to back slightly ahead of the trough and veer markedly behind it. Apart from showers moving through the Cheshire Gap, and reaching as far south as Benson (Oxon), shower activity seemed to be confined to the trough line.

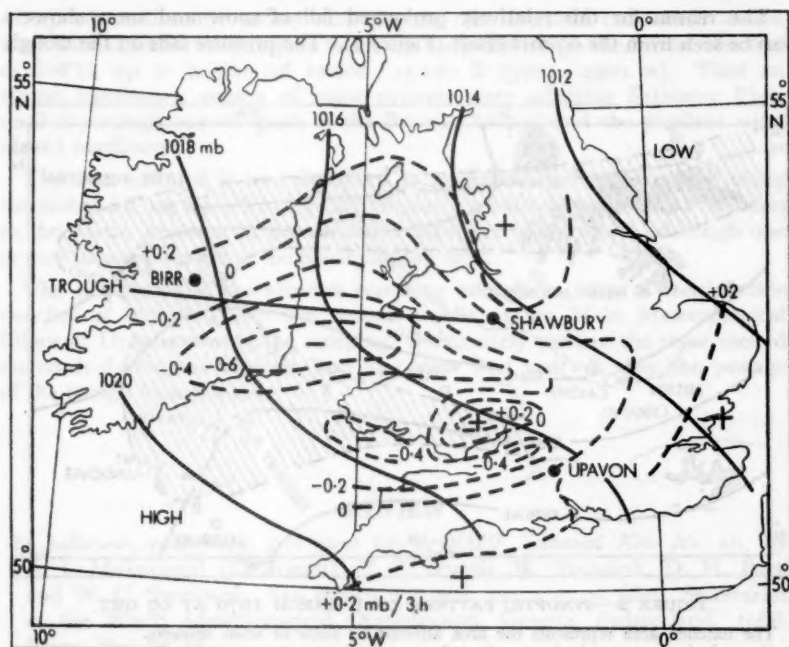* 1 inch ≈ 2·5 cm. 1 knot ≈ 0·5 m/s.

FIGURE I—SYNOPTIC PATTERN ON 6 MARCH 1970 AT 06 GMT

+ rising barometer   – falling barometer
————— isobars   – – – – isallobars at intervals of 0·2 mb/3 h

This is shown by the observations from Little Rissington some 35 nautical miles (approximately 65 km) due north of Upavon, and well protected by the Welsh mountains (Table I).

TABLE I—HOURLY OBSERVATIONS AT LITTLE RISSINGTON ON 6 MARCH 1970

Time (GMT)	07	08	09	10	11	12
Wind (deg/kt)	290/08	250/07	270/08	280/08	280/11	280/09
Weather	Nil	Light snow shower	Recent snow shower	Nil	Nil	Nil

Table II gives the observations for Upavon on Salisbury Plain. A snow shower commenced at 0830 GMT some 35 nautical miles ahead of the trough. Snow or snow showers continued with varying intensity until 1230 GMT. With the passage of the trough the surface wind veered to 330° and the precipitation stopped.

TABLE II—HOURLY OBSERVATIONS AT UPAVON ON 6 MARCH 1970

Time (GMT)	08	09	10	11	12	13
Wind (deg/kt)	290/02	320/08	300/05	320/05	290/05	310/08
Weather	Nil	Moderate snow shower	Snow grains	Slight snow	Moderate snow	Recent snow

282   *Meteorological Magazine*, **99**, 1970

The reason for this relatively prolonged fall of snow and snow showers can be seen from the 09 GMT chart (Figure 2). The pressure falls on the trough
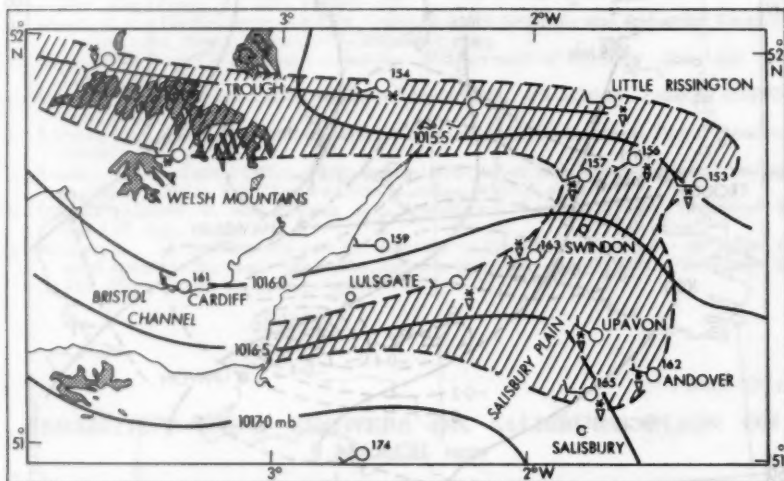

FIGURE 2—SYNOPTIC PATTERN ON 6 MARCH 1970 AT 09 GMT

The hatched area represents the area affected by snow or snow showers.
Ground above 400 m is shown stippled.

and over the Bristol Channel had combined to back the gradient wind ahead of the trough until it flowed along the Bristol Channel straight to Salisbury Plain. At this time an aircraft reported cumulus cloud tops at 12 000 ft (about 3700 m) over Salisbury Plain. As can be seen from Figure 3, the 06 GMT
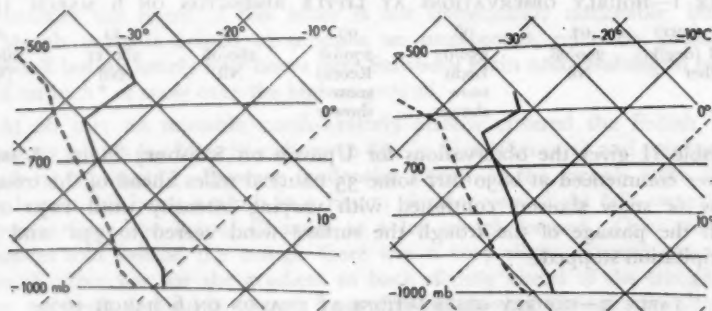
(a) Larkhill 09 GMT   (b) Aberporth 06 GMT

FIGURE 3—RADIOSONDE ASCENTS FOR 6 MARCH 1970

————. Dry-bulb temperature   .— — — —. Dew-point temperature

Aberporth radiosonde ascent and the 09 GMT Larkhill radiosonde ascent were both unstable with respect to the sea temperatures in the Bristol Channel of 6–8°C, up to heights of 12 000 – 14 000 ft (3700 – 4300 m). Thus an almost continuous stream of snow showers were affecting Salisbury Plain until the trough moved south of the Bristol Channel and the gradient wind veered north-west.

The area affected is best described as a pear-shaped zone centred along the isobar for 1016.5 mb at 09 GMT (Figure 2), extending almost to Swindon in the north, Andover in the east, and Salisbury in the south, although one or two showers did reach the Southampton area.

The persistence of the showers was long enough to cause a considerable number of inquiries from the general public at the Main Meteorological Office at Upavon during the morning. Fortunately most of the snow melted on roads during the showers, and any snow that was left after the passage of the trough soon thawed.

REVIEW

Air pollutants, meteorology, and plant injury, WMO Technical Note No. 96, by E. I. Mukammal (Chairman), C. S. Brandt, R. Neuwirth, D. H. Pack and W. C. Swinbank. 210 mm × 275 mm, pp. x + 73, *illus.*, Secretariat of the World Meteorological Organization, Geneva, Switzerland, 1968. Price: Sw. Fr. 10.–.

This WMO *Technical Note* has been published at a time when environmental problems have suddenly become a part of political consciousness on an international scale. In the scientific context of its authors, and most readers, it is a literature review of the broad and complex subject of the interactions between plants and pollutants of their environment. At the same time the note is a statement by an authoritative international body of the present knowledge, and lack of knowledge, in the field, as well as the prospects for forecasting and control of pollutants, and should be reading matter for political advisers on environmental problems. The authors have faced a difficult task simply because of the range of topics covered and as a consequence their work shows some disparity in the level of treatment between sections. Chapter 4, on the physiology of injury by pollutants, and Chapter 5, which catalogues the symptoms of injury of plant species by major pollutants *and* other possible causes of similar symptoms, are probably of greatest practical value. Chapter 7, on sampling methods and Chapter 8, which considers control methods, are also useful reviews of the fields concerned. The major criticisms must be of Chapter 6. It seems inappropriate in a publication of this level to reprint five pages (sections 6.1 – 6.4) of a general discussion of air pollution meteorology, however good in its original context.* This must surely be familiar ground to most readers of the note, and the original journal is easily accessible to others. Similarly the mathematical treatment of turbulent exchange at the air–crop interface (section 6.7) is presented adequately in many quite

* PACK, D. H.; Meteorology of air pollution. *Science, Washington*, **146**, 1964, pp. 1119–1128.

elementary textbooks, and it should hardly warrant more than a note on the
limitations of its validity. This space could surely have been more usefully
employed to present a separate discussion of the difficult problem of the
deposition of pollutants on vegetation and other surfaces. In particular I
am surprised that no reference is made to the more recent papers on deposition
by A. C. Chamberlain (e.g. in *Proc. R. Soc., London*, A, 1966, **290**, pp. 236–265
and **296**, pp. 45–70. In a publication of this nature omissions are inevitable,
but do not detract from the value of this attempt to tie together the threads
of this vitally important and fascinating subject.

<div align="right">J. A. CLARK</div>

NOTES AND NEWS

<div align="right">551.575.1:551.578.46</div>

Shallow fog over a snow surface

At Machrihanish, Kintyre, Argyll, shallow fog, with visibility not more
than 500 yd, started to form at 0730 GMT on 15 February 1970 over a snow
surface and persisted until 1115 GMT reaching a height of 2–4 metres (see
Plate IV). Visibility above the fog was 20 miles or more. Snow of a fine dry
texture had fallen for about nine hours during the night to give an average
depth of 7 cm with considerable drifting. The snowfall ceased at 0620 GMT
and the sky cleared about 07 GMT. During the next few hours the wind was
calm or very light and the sky was almost cloudless. Air temperature in the
screen fell rapidly from − 0·8°C at 07 to − 7·1°C at 09 GMT with an absolute
minimum reading of − 8·0°C.

Time GMT	06	07	08	09	10	11	12
				degrees Celsius			
Dry bulb	+0·1	− 0·8	− 3·5	− 7·1	− 4·0	− 1·8	0·0
Ice bulb	0·0	− 1·2	− 3·5	− 7·1	− 4·0	− 2·1	− 0·9

<div align="right">V. C. SANDERS</div>

OBITUARY

It is with regret that we have to record the death on 27 May 1970 of Mr
W. H. Betts, Radio (Meteorological) Technician.

HONOUR

The following honour was announced in the Queen's Birthday Honours
List 1970 :

<div align="center">I.S.O.</div>

Mr A. F. Jenkinson, Head of Flood Investigation Section, Meteorological
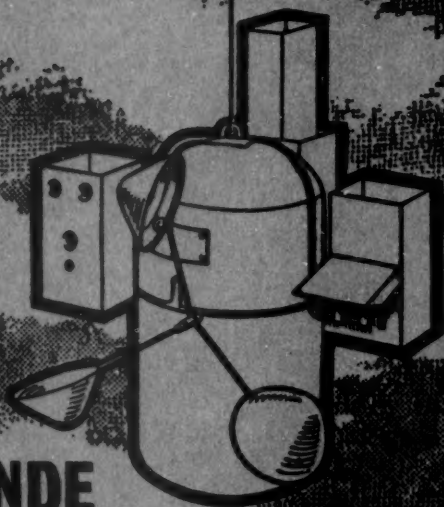Office, Bracknell.

CORRECTIONS

Meteorological Magazine, June 1970, p. 158.

In equation (1) the final term on the left-hand side should read $\dfrac{\partial^2 \psi}{\partial x^2}$.

In equation (2) for the term $(l^2 + k^2)$ read $(l^2 - k^2)$.

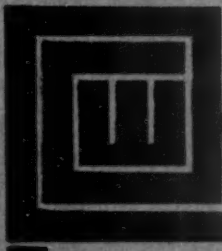In the fourth line of the fourth paragraph for 'gets' read 'sets'.

CONTENTS

NOTICES

It is requested that all books for review and communications for the Editor be addressed to the Director-General, Meteorological Office, London Road, Bracknell, Berkshire, RG12 2SZ, and marked 'for Meteorological Magazine.'

The responsibility for facts and opinions expressed in the signed articles and letters published in this magazine rests with their respective authors.

All inquiries relating to the insertion of advertisements in the Meteorological Magazine should be addressed to the Director of Publications, H.M. Stationery Office, Atlantic House, Holborn Viaduct, London E.C.1. (Telephone: 01-248 9876, extn 6098).

The Government accepts no responsibility for any of the statements in the advertisements appearing in this publication, and the inclusion of any particular advertisement is no guarantee that the goods advertised therein have received official approval.